ANALYZING LOAD RESPONSE OF INTERCONNECTED VECTOR CONTROLLED DFIG WITH SEIG AND SYNCHRONOUS GENERATOR

Ramkumar. A[1] and Durairaj. S[2]
[1]Research Scholar/Dept. of EEE, Kalasalingam University, Srivilliputhur, Tamil Nadu, India
[2]Professor/Dept. of EEE, Kings College of Engineering, Tanjore, Tamil Nadu, India

ABSTRACT
Now a days, due to the increase of electrical energy requirement, the renewable energy sources such as hydro, solar and wind are used to produce the electrical energy. Compared to the other renewable sources, wind energy conversion system (WECS) is more efficient and economical. In this paper, assessments of interconnection of Doubly-Fed Induction Generator (DFIG), Self-Excited Induction Generator (SEIG) and Hydro-Governor Synchronous Generator with various loads like R, L, C, RL, RLC are discussed. Analysis of those generators with the different load conditions are carried out using PSCAD/EMTDC software. From the simulations results, some of the recommendations and suggestions have been extracted.

KEYWORDS: *Doubly Fed Induction Generator (DFIG), Self-Excited Induction Generator (SEIG), Hydro- Governor Synchronous Generator.*

NOMENCLATURE

P_{Hydro}	Electric power generated by the hydro plant
$Q,, H, \eta$	Discharge through hydro turbine (m^3/s), water head in metre, hydro system efficiency (%)

DFIG parameters

V_{qs}, V_{ds},	Supply voltages in *dq* reference frame
V_{qr}, V_{dr}	Rotor voltages in *dq* reference frame
λ_{qs}, λ_{ds},	Stator flux linkages in *dq* reference frame
λ_{qr}, λ_{dr}	Rotor flux linkages in *dq* reference frame
T_e	Electromagnetic torque
P_{DFIG},Q_{DFIG}	Active[MW] and reactive[Mvar] powers

SEIG parameters

R_s, R_r	Stator resistance [p.u.], rotor resistance [p.u.]
X_s, X_{lr}, X_m	Stator reactance [p.u.], rotor leakage reactance [p.u.], magnetizing reactance [p.u.]
Y_s, Y_r, Y_m	Stator admittance [p.u.], rotor admittance [p.u.], magnetizing admittance [p.u.]
$f_{p.u.}$	Frequency in p.u.
P_{SEIG},Q_{SEIG}	Active[MW] and reactive[Mvar] powers

Synchronous Generator parameters

v_d, v_q, v_{fd}, , E_f	Armature *d*-axis terminal voltage, armature *q*-axis terminal voltage, field winding terminal voltage, field excitation voltage
i_d, i_q, i_{fd}, i_{kd} i_{kq}, I_f	Armature *d*-axis terminal current, armature *q*-axis terminal current, field winding terminal current, *d*-axis damper winding current, *q*-axis damper winding current, field current
L_d, L_{ls}, L_{md} L_{lfd}, L_{lkd}, L_{mq} L_{lkq}	Self inductance in *d*-axis [p.u.], armature phase leakage inductance [p.u.], *d*- axis coupling inductance [p.u.], field winding leakage inductance [p.u.], *d*-axis damper winding leakage inductance [p.u.], *q*-axis coupling inductance [p.u.], *q*-axis damper winding leakage inductance [p.u.]
P_{SYN}, Q_{SYN}	Active[MW] and reactive[Mvar] powers

I. INTRODUCTION

Renewable energy generation system, such as wind energy conversion is mainly used in offshore remote areas. Induction generator which is operated at fixed and variable speeds are used to produce the electrical energy. By using the power electronic converters, capturing better energy is possible from the variable speed generator than the fixed speed generator. Negative slip operating region of the squirrel cage induction machine is called as self-excited induction generator (SEIG) and it is the most suitable one in an isolated system. At the stator terminal, the excitation capacitor is connected and is used to build the voltage at rated level.

Without proper reactive power compensation of wind energy conversion system, enough real power cannot be supplied. It is essential to move active power through the transmission and distribution systems. Lag of reactive power leads to voltage sag, voltage imbalance and voltage distortion. It also weakens the transmission network.

Doubly-fed induction generator (DFIG) is one of the most popular variable speed induction generators and the power is taken from both stator and rotor. It is the most suitable are in the large amount of electric power generation. The electrical power which is produced in the rotor is only slip power and its voltage magnitude and frequency are less than the rated value. Those values can be improved upto the rated level by changing the firing angle of rotor power semiconductor devices [1]. Functions of grid and rotor side converters are described in [2]-[8].

Another most popular renewable energy generation is hydro power electrical energy generation. The electric power generated by the hydro power is proportional to the product of net head in metre and flow of water in cubic metre per second.

$$P_{Hydro} = 9.81QH\eta \tag{1}$$

In practice, interconnected generators such as asynchronous and synchronous generators meet the load demand. In this paper, behaviour of asynchronous and synchronous generators performance and load response of those interconnected generators are analyzed. Mathematical modelling and designing of asynchronous and synchronous generators are discussed. Investigation on the behavior of real and reactive power flows of interconnected vector controlled DFIG and SEIG with the hydro-governor synchronous generator at the various load conditions is presented in the following section.

II. MATHEMATICAL MODELLING OF MACHINES

2.1 DFIG

Wound rotor induction machine model is similar to fixed-speed induction generator model and the mathematical equations of DFIG [9]-[11] with respect to *dq* are as follows: Stator and rotor voltages as well as real and reactive power equations are obtained from stator reference frame as expressed in eqns. (2)-(7):

$$V_{qs} = p\lambda_{qs} + \omega\lambda_{ds} + r_s i_{qs} \tag{2}$$

$$V_{ds} = p\lambda_{ds} - \omega\lambda_{qs} + r_s i_{ds} \tag{3}$$

$$V_{qr} = p\lambda_{qr} + (\omega - \omega_r)\lambda_{dr} + r_r i_{qr} \quad (4)$$

$$V_{dr} = p\lambda_{dr} - (\omega - \omega_r)\lambda_{qr} + r_r i_{dr} \quad (5)$$

$$P_{DFIG} = \frac{3}{2}\left(V_{ds} i_{ds} + V_{qs} i_{qs}\right) \quad (6)$$

$$Q_{DFIG} = \frac{3}{2}\left(V_{qs} i_{ds} - V_{ds} i_{qs}\right) \quad (7)$$

Stator and rotor flux linkage equations are:

$$\lambda_{qs} = (L_{ls} + L_m) i_{qs} + L_m i_{qr} \quad (8)$$

$$\lambda_{ds} = (L_{ls} + L_m) i_{ds} + L_m i_{dr} \quad (9)$$

$$\lambda_{qr} = (L_{lr} + L_m) i_{qr} + L_m i_{qs} \quad (10)$$

$$\lambda_{dr} = (L_{lr} + L_m) i_{dr} + L_m i_{ds} \quad (11)$$

Based on the flux linkage eqns. (8)-(11), T_e is written in form of:

$$T_e = -\frac{3}{2}\frac{P}{2}\left(\lambda_{ds} i_{qs} - \lambda_{qs} i_{qs}\right) \quad (12)$$

2.2. SEIG

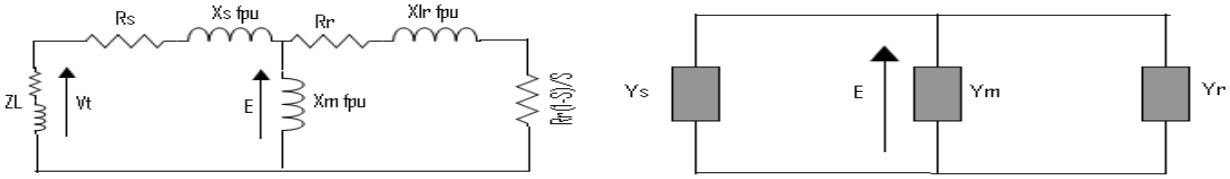

(a) (b)

Figure 1. Equivalent circuit of the induction machine a) steady-state equivalent circuit b) equivalent circuit represented in terms of admittance

Figure 1(a) and 1(b) shows the equivalent circuit of induction machine [12], [13]. From these equivalent circuits, stator, rotor and magnetizing admittances are derived:

$$Y_s = R_e(Y_s) + jI_m(Y_s) \quad (13)$$

$$Y_r = \frac{\frac{R_r}{s}}{\left(\frac{R_r}{s}\right)^2 + (X_{lr} f_{pu})^2} - j\frac{X_{lr} f_{pu}}{\left(\frac{R_r}{s}\right)^2 + (X_{lr} f_{pu})^2} \quad (14)$$

$$Y_m = -j\frac{1}{X_m} \quad (15)$$

By solving the eqns. (13)-(15), real and reactive parts of the induction machine is given as follows:

$$R_e(Y_s) + \frac{\frac{R_r}{s}}{\left(\frac{R_r}{s}\right)^2 + (X_{lr} f_{pu})^2} = 0 \quad (16)$$

$$I_m(Y_s) + \frac{X_{lr} f_{pu}}{\left(\frac{R_r}{s}\right)^2 + (X_{lr} f_{pu})^2} + \frac{1}{X_m f_{pu}} = 0 \quad (17)$$

2.3. Synchronous Machine

Based on the state space representation, the mathematical modeling of synchronous machine [14]-[16] with the rotating *dq* reference frame is expressed as follows.

$$\left[\dot{\mathbf{I}}\right] = [L]^{-1}[V] - [L]^{-1}[R][I] \tag{18}$$

Where:

$$[I] = \begin{bmatrix} i_d \\ i_q \\ i_{fd} \\ i_{DK} \\ i_{QK} \end{bmatrix} \quad [V] = \begin{bmatrix} v_d \\ v_q \\ v_{fd} \\ 0 \\ 0 \end{bmatrix} \tag{19}$$

$$[L] = \begin{bmatrix} -(L_{ls}+L_{md}) & 0 & L_{md} & L_{md} & 0 \\ 0 & -(L_{ls}+L_{md}) & 0 & 0 & L_{md} \\ -L_{md} & 0 & (L_{lfd}+L_{md}) & L_{md} & 0 \\ -L_{md} & 0 & L_{md} & (L_{lKd}+L_{md}) & 0 \\ 0 & -L_{mq} & 0 & 0 & (L_{lKq}+L_{mq}) \end{bmatrix} \tag{20}$$

Mathematical equations for the self and mutual inductances are represented as:

$$\begin{aligned} L_d &= L_{ls} + L_{md}, \\ L_q &= L_{ls} + L_{mq}, \\ L_f &= L_{lfd} + L_{md}, \\ L_D &= L_{lKd} + L_{md}, \\ L_Q &= L_{lKq} + L_{mq}, \\ M_{fD} &= L_{md}, \\ M_{dD} &= L_{md}, \\ M_{qQ} &= L_{mq} \end{aligned} \tag{21}$$

III. INTERCONNECTED ASYNCHRONOUS AND SYNCHRONOUS GENERATORS

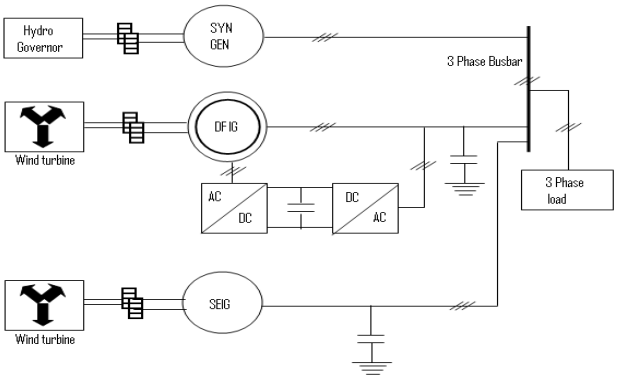

Figure 2. Interconnected DFIG, SEIG with Synchronous Generator

Interconnection of asynchronous and synchronous machines for sharing the three phase load is constructed using PSCAD simulation tool and it can be seen in Figure 2. During the interconnection, magnitude of voltage, phase sequence and frequency of those machines should be maintained at constant value. This is achieved only by the controlling aspects of hydro governor in synchronous generator and the speed of the asynchronous machine rotating part should be maintained at proper value by adjusting the speed of the wind turbine.

IV. SIMULATION SETUP OF ASYNCHRONOUS AND SYNCHRONOUS GENERATORS

Design of DFIG, SEIG and Synchronous generator are done by using PSCAD is follows.

4.1. DFIG

DFIG is constructed [17], [18] by the PSCAD simulation tool. Designing of rotor circuit converter unit is having some important steps such as rotating magnetic flux vector location, Generation of rotor phase reference currents and Current Reference Pulse Width Modulator (CRPWM) Converter.

4.1.1. Rotating magnetic Flux vector location

Three phase stator voltages V_a, V_b and V_c are converted into V_α and V_β by using 3 to 2 transformation. With the transfer function of $\frac{G(sT)}{1+sT}$, V_α and V_β are converted into polar form is shown in fig. 3.

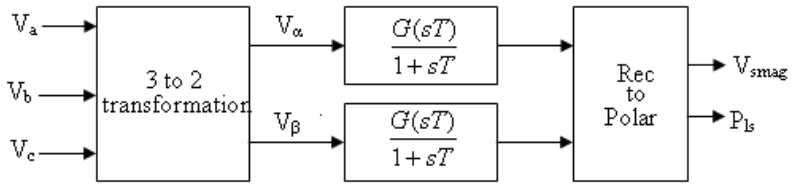

Figure 3. Rotating Flux vector location

3 to 2 transformation is denoted as eqn. (22):

$$\begin{pmatrix} V_\alpha \\ V_\beta \end{pmatrix} = \frac{2}{3}\begin{pmatrix} 1 & -1/2 & -1/2 \\ 0 & \sqrt{3}/2 & \sqrt{3}/2 \end{pmatrix}\begin{pmatrix} V_a \\ V_b \\ V_c \end{pmatrix} \tag{22}$$

By using clarke components, λ_α and λ_β are obtained from the integration of V_α and V_β shown in eqn. (23).

$$|\lambda| = \sqrt{\lambda_\alpha{}^2 + \lambda_\beta{}^2}, \phi_s = \tan^{-1}(\lambda_\beta / \lambda_\alpha) \tag{23}$$

4.1.2. Generation of rotor phase reference currents

Generation of rotor phase reference currents i_{ra_ref}, i_{rb_ref} and i_{rc_ref} are shown in Fig. 4.

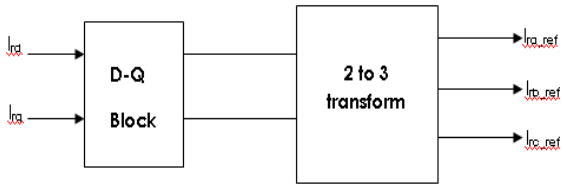

Figure 4. Generation of rotor phase reference currents

Fig. 4 shows that, rotor phase reference currents i_{ra_ref}, i_{rb_ref} and i_{rc_ref} are generated by *dq* and *2 to 3* transformations. The eqns.(24), (25) are the mathematical representation of those transformations.

$$\begin{bmatrix} \alpha \\ \beta \end{bmatrix} = \begin{bmatrix} \cos\theta & -\sin\theta \\ \sin\theta & \cos\theta \end{bmatrix}\begin{bmatrix} d \\ q \end{bmatrix} \tag{24}$$

$$\begin{bmatrix} a \\ b \\ c \end{bmatrix} = \begin{bmatrix} 1 & 0 \\ -1/2 & \sqrt{3}/2 \\ -1/2 & -\sqrt{3}/2 \end{bmatrix}\begin{bmatrix} \alpha \\ \beta \end{bmatrix} \tag{25}$$

4.1.3. Current Reference Pulse Width Modulator (CRPWM) Converter

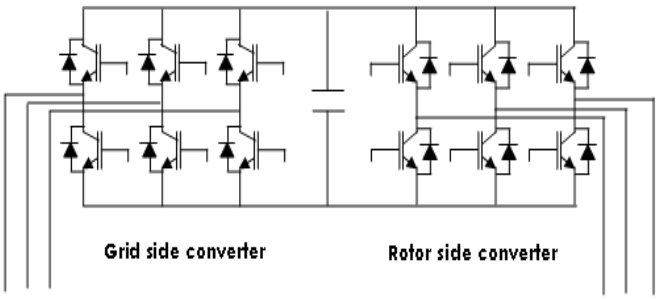

Figure 5. CRPWM Converter

Fig. 5 shows that, current reference pulse width modulator (CRPWM) of the DFIG. A dc capacitor which is connected between grid and rotor side converters is used to keep the smooth DC voltage and also remove the ripple. DC voltage across the capacitor is maintained at a constant value.

4.2. Synchronous Machine

Fig.6 shows the modelling of synchronous machine [17], [18] with solid state exciter and hydro governor by using PSCAD/EMTDC.

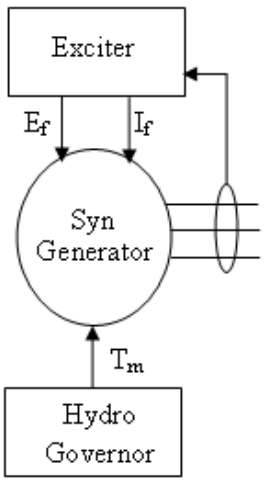

Figure 6. Modelling of Synchronous machine

Field winding of the synchronous generator is excited by solid state exciter *(SSE)* and hydro-governor gives the mechanical torque T_m to the generator [10], [11]. Field current I_f and excitation voltage E_f are controlled by the exciter and mechanical torque T_m is controlled by the hydro governor system.

4.3. SEIG

Modelling of SEIG [17], [18] by PSCAD is shown in fig. 7. It is having two major systems such as wind turbine governor and modelling of wind turbine shown in section 4.3.1.

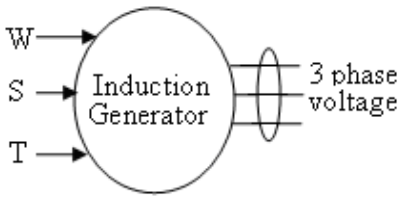

Figure 7. Modelling of SEIG

4.3.1. Wind Turbine Governor and Model

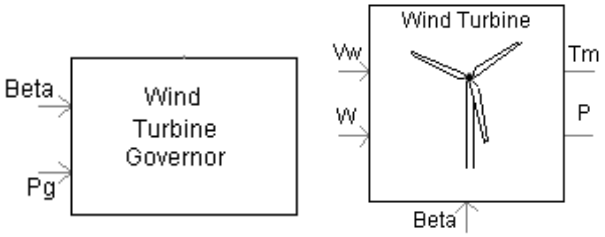

(a) (b)

Figure 8. (a) Wind turbine governor and (b) Wind turbine model of SEIG

Fig. 8 (a) shows the wind turbine governor system. P_g and *beta* are the parameters of the governor system. Based on P_g and *beta* the wind turbine governor is controlled. Fig.8 (b) shows the model for wind turbine. Wind speed V_w, mechanical speed of the machine *w* and pitch angle of the turbine blades is *beta* are given to the wind turbine. Those inputs control the output torque T_m and power *P* of the wind turbine.

V. SIMULATION RESULTS

Interconnected vector controlled DFIG, SEIG with hydro-governor synchronous generator are developed using PSCAD. Simulation results for various load conditions of interconnected system are obtained by the variation of load such as *R, L, C, RL, RLC* and the responses of real and reactive powers P_{DFIG}, P_{SYN}, P_{SEIG} and Q_{DFIG}, Q_{SYN}, Q_{SEIG} respectively are observed. Based on the performance of those generators, selection of generators will be made with respect to the various load conditions.

5.1. Case-I: Resistive load

Table 1. Real and reactive powers of interconnected generators during resistive load conditions

Load	DFIG				Synchronous Generator				SEIG			
	Initial state (0-0.5sec)		Steady state		Initial state (0-0.5sec)		Steady state		Initial state (0-0.5sec)		Steady state	
	P_{DFIG} (MW)	Q_{DFIG} (Mvar)	P_{DFIG} (MW)	Q_{DFIG} (Mvar)	P_{SYN} (MW)	Q_{SYN} (Mvar)	P_{SYN} (MW)	Q_{SYN} (Mvar)	P_{SEIG} (MW)	Q_{SEIG} (Mvar)	P_{SEIG} (MW)	Q_{SEIG} (Mvar)
25% load	700	360	54.18	62.23	52 to 112	-60 to 90	44.94	-24.84	0 to -245	0 to -415	102.5	-59.34
50% load	700	320	56.83	59.67	52 to 108	-50 to 100	111.2	104.8	0 to -230	0 to -390	102.3	-59.59
75% load	695	345	54.67	60	60 to 112.5	-25 to 104	187.1	213.8	0 to -220	0 to -370	102.3	-60.15
100% load	690	295	56.6	55.69	40 to 75	0 to 106	270.2	310.1	0 to -210	0 to -350	101.9	-60.69

Response of real and reactive powers of the interconnected system with the various stage of resistive load is shown in Table 1. At the initial condition, the maximum variation of P_{DFIG} of the DFIG goes to 690 at full load and 700MW at 50% and 25% load. After 0.5 sec, it comes to steady state level are 56.6MW, 54.67MW, 56.83MW and 54.18MW at 100%, 75%, 50% and 25% of resistive loads respectively. Peak value of Q_{DFIG} goes to 295 at full load, 360Mvar at 25% load within 1sec. It has steady state range with 55.69Mvar, 60Mvar, 59.67Mvar and 62.23Mvar at from 100% to 25% full load resistive load conditions.

In the synchronous generator, settling time of steady state level of P_{SYN} depends upon the load conditions. At the initial condition, fluctuation of P_{SYN} is more and its steady state ranges are 270.2MW, 187.1MW, 111.2MW and 44.94MW at 100%, 75%, 50% and 25% of resistive load respectively. After 0.5 sec, the fluctuation of Q_{SYN} vanishes. The settling times of synchronous generator Q_{SYN} are 4sec and 3sec with respect to full load to 25% load conditions. Steady state ranges of Q_{SYN} are 310.1Mvar, 213.8Mvar, 104.8Mvar and -24.84Mvar at the 100% to 25% resistive load. At 25% load, the synchronous generator consumes Q_{SYN} and its value is -24.84Mvar.

At the initial state, maximum values of P_{SEIG} and Q_{SEIG} are -245MW and -415Mvar respectively. Settling time of P_{SEIG} and Q_{SEIG} comes within 2.0sec at different conditions of resistive loads. After 2.0sec, the SEIG steady state value of P_{SEIG} and Q_{SEIG} are 101.9MW, 102.3MW, 102.3MW, 102.5MW, and -60.69Mvar, -60.15Mvar, -59.59Mvar and -59.34 Mvar at resistive load from 100% to 25% resistive load. Based on the above results, SEIG consumes Q_{SEIG} at all the resistive load conditions.

During the steady state condition, with the different stages of resistive load, the changes in ranges of P_{DFIG} and Q_{DFIG} are small, that is, 2.65 MW from 54.18 to 56.83 MW and 6.54 Mvar from 55.69 to 62.23 Mvar. But P_{SYN} has 225.26 MW from 44.94 MW to 270.2 MW and Q_{SYN} is 334.94 Mvar from -24.84 to 310.1 Mvar. Similarly, P_{SEIG} and Q_{SEIG} changes in values are 0.6 MW from 101.9 to 102.5 MW and -1.35 Mvar from-59.34 to -60.69 Mvar. Based on the overall performance of the interconnected generators with the resistive load, fluctuation of real and reactive powers of the synchronous generator at steady state is larger than the asynchronous generators. SEIG consumes the Q_{SEIG} at all the loads.

5.2. Case- II: Inductive load

Table 2. Real and reactive powers of interconnected generators during inductive load conditions

Load	DFIG				Synchronous Generator				SEIG			
	Initial state (0-0.5sec)		Steady state		Initial state (0-0.5sec)		Steady state		Initial state (0-0.5sec)		Steady state	
	P_{DFIG} (MW)	Q_{DFIG} (Mvar)	P_{DFIG} (MW)	Q_{DFIG} (Mvar)	P_{SYN} (MW)	Q_{SYN} (Mvar)	P_{SYN} (MW)	Q_{SYN} (Mvar)	P_{SEIG} (MW)	Q_{SEIG} (Mvar)	P_{SEIG} (MW)	Q_{SEIG} (Mvar)
25% load	640	380	58.01	64.97	-10 to 80	-60 to 90	8.066	-124.0	0 to 250	0 to -420	102.9	-59.26
50% load	650	380	51.84	64.99	-16 to 76	-60 to 90	6.186	-121.8	0 to 260	0 to -415	102.9	-59.62
75% load	660	380	56.11	64.32	-14 to 64	-65 to 90	9.252	-92.66	0 to 270	0 to -405	102.7	-59.48
100% load	685	380	55.98	63.45	-20 to 57	-65 to 95	12.44	-54.12	0 to 280	0 to -400	102.6	-59.51

Performances of DFIG, SEIG and hydro-governor synchronous generator with the inductive load are shown in Table 2. The initial value of P_{DFIG} of the DFIG within the duration of 0.5sec is 640 at 25% load to 685MW at full load. After this period, the P_{DFIG} comes to steady state such as 55.98MW at full load; 56.11MW at 75% load; 51.84MW at 50% load; 58.01MW at 25% load. P_{DFIG} variation of the DFIG is minimum because of the changes in values of P_{DFIG} from 51.84MW to 58.01MW. At the initial state, Q_{DFIG} is 380Mvar and it comes down to steady state 1sec. Q_{DFIG} steady state values are 63.45Mvar, 64.32Mvar, 64.99Mvar and 64.97Mvar at 100%, 75%, 50% and 25% inductive load.

Peak values of P_{SYN} and Q_{SYN} can be obtained within 0.5sec and the maximum values go to 80MW at 25% load. Steady state values of P_{SYN} are 12.44MW, 9.252MW, 6.186MW, 8.066MW at various inductive loads from 100% to 25% respectively. The generation of P_{SYN} at the inductive load is comparatively low than the resistive load. Similarly the steady state values of Q_{SYN} are -54.12Mvar, -92.66Mvar, -121.8Mvar, -124.0Mvar at 100% to 25% load. Based on the above results, it is identified that, synchronous generator consumes Q_{SYN} and this consumption increases from lower to higher load.

At the initial state, maximum values of P_{SEIG} and Q_{SEIG} are 280MW at full load and -420Mvar at 25% load. Settling time of both the power P_{SEIG} and Q_{SEIG} reaches within 2.0sec and steady-state values of P_{SEIG} and Q_{SEIG} are 102.6MW, 102.7MW, 102.9MW, 102.9MW and -59.51Mvar, -59.48Mvar, -59.62Mvar, -59.26Mvar at 100% to 25% load. From this simulation results, SEIG consumes Q_{SEIG} and its consumption rate varies from -59.26Mvar to -59.62Mvar with the different inductive loads.

Based on the above discussions, overall performance of P_{DFIG} and Q_{DFIG} is consistent, that is, variation of their powers are minimum and their values are 6.17MW from 51.84 MW to 58.01 MW and 1.54 Mvar from 63.45 to 64.99 Mvar. But the performance of synchronous generator differs from the case I. It is noted that, changes in P_{SYN} and Q_{SYN} at steady state are 6.254 MW from 6.186 to

12.44 MW and -69.88 Mvar from -124.0 Mvar to -54.12 Mvar respectively. At the different stages of inductive load, P_{SEIG} and Q_{SEIG} steady states are 0.3 MW from 102.6 MW to 102.9 MW and -0.36 Mvar from -59.26 to -59.62 Mvar respectively.

5.3. Case-III: Capacitive load

Table 3. Real and reactive powers of interconnected generators during capacitive load conditions

Load	DFIG				Synchronous Generator				SEIG			
	Initial state (0-0.5sec)		Steady state		Initial state (0-0.5sec)		Steady state		Initial state (0-0.5sec)		Steady state	
	P_{DFIG} (MW)	Q_{DFIG} (Mvar)	P_{DFIG} (MW)	Q_{DFIG} (Mvar)	P_{SYN} (MW)	Q_{SYN} (Mvar)	P_{SYN} (MW)	Q_{SYN} (Mvar)	P_{SEIG} (MW)	Q_{SEIG} (Mvar)	P_{SEIG} (MW)	Q_{SEIG} (Mvar)
25% load	690	398	52.9	66.98	0 to 122	-77 to 94	11.19	-128.6	0 to -260	0 to -432	102.8	-59.43
50% load	690	397	55.79	65.82	0 to 125	-77 to 90	12.63	-129.3	0 to -260	0 to -434	102.8	-58.75
75% load	690	394	53.49	66.19	0 to 143	-77 to 80	13.88	-130.5	0 to -260	0 to -440	103.1	-58.99
100% load	695	390	54.27	65.89	0 to 150	-77 to 77	15.12	-130.8	0 to -260	0 to -450	102.8	-59.19

From the Table 3, peak value of P_{DFIG} of DFIG is 690MW at 75%, 50%, 25% load and 695MW at full load and Q_{DFIG} peak value is 398 Mvar at 25% of capacitive load. Settling time of both the powers of DFIG is within 1sec. After the settling time, the steady state levels of P_{DFIG} and Q_{DFIG} are 54.27MW, 53.49MW, 55.79MW, 52.9MW and 65.89Mvar, 66.19Mvar, 65.82Mvar, 66.98Mvar at the capacitive loads of 100%, 75%, 50%, and 25% full load conditions respectively.

From the duration 0.1 to 0.5sec, the fluctuation of both the powers P_{SYN} and Q_{SYN} are 150MW at full load and 94Mvar at 25% load. Steady state value is reached in 3sec and P_{SYN} and Q_{SYN} of synchronous generator are 15.12MW, 13.88MW, 12.63MW, 11.19MW and -13.8Mvar, -130.5Mvar, -129.3Mvar, -128.6Mvar at the load range of 100% to 25% capacitive load respectively.

At the initial time period from 0 to 0.5sec, P_{SEIG} and Q_{SEIG} have -260MW in all load conditions and -450Mvar at full load. The settling time of P_{SEIG} and Q_{SEIG} reached in 2.0sec. The steady state value of SEIG are 102.8MW, 103.1MW, 102.8MW, 102.8MW and-59.19Mvar, -58.99Mvar, -58.75Mvar, -59.43Mvar from 100% to 25% capacitive load respectively.

Change in values of P_{DFIG} and Q_{DFIG} at the different range of capacitive load conditions are minimum. Their values are 2.89MW from 52.9 to 55.79MW, 1.16Mvar from 65.82 to 66.98Mvar. From the above discussion, delivering P_{SYN} is minimum (11.19 to 15.12MW at 25% to full load) and also the synchronous generator consumes Q_{SYN}. Variation of P_{SEIG} and Q_{SEIG} are minimum, that is, change in values of P_{SEIG} is 0.3MW from 102.8 to 103.1MW and Q_{SEIG} is -0.68Mvar from -59.43 to -58.75Mvar and SEIG delivers P_{SEIG} and consumes Q_{SEIG}. Both in inductive and capacitive loads, P_{SYN} is minimum and consumes Q_{SYN}. The performance of DFIG is consistent and SEIG contributes real power and consumes reactive power.

5.4. Case-IV: RL load

Table 4. Real and reactive powers of interconnected generators during RL load conditions

Load	DFIG				Synchronous Generator				SEIG			
	Initial state (0-0.5sec)		Steady state		Initial state (0-0.5sec)		Steady state		Initial state (0-0.5sec)		Steady state	
	P_{DFIG} (MW)	Q_{DFIG} (Mvar)	P_{DFIG} (MW)	Q_{DFIG} (Mvar)	P_{SYN} (MW)	Q_{SYN} (Mvar)	P_{SYN} (MW)	Q_{SYN} (Mvar)	P_{SEIG} (MW)	Q_{SEIG} (Mvar)	P_{SEIG} (MW)	Q_{SEIG} (Mvar)
25% load	682	305	55.84	62.5	0 to 78	-40 to 88	35.12	-39.8	0 to -245	0 to -408	102.6	-59.38
50% load	682	305	54.54	61.85	0 to 80	-50 to 100	81.66	79.99	0 to -230	0 to -380	102.5	-59.71
75% load	685	305	54.26	60.09	0 to 80	-25 to 115	130.8	186.2	0 to -220	0 to -365	102.2	-60.04

100% load	685	310	57.01	57.7	0 to 80	0 to 120	188.4	292.2	0 to -210	0 to -350	102.0	-60.41

Behavior of interconnected generators with *RL load, 0.8pf* is shown in Table 4. At the initial condition, P_{DFIG} immediately reaches 682 at 25% load and 685MW at full load. It comes to normal value before 1sec, that is, its steady state values are 57.01MW, 54.26MW, 54.54MW, 55.84MW at 100%, 75%, 50%, 25% RL load. Similarly the Q_{DFIG} values are 57.7Mvar, 60.09Mvar, 61.85Mvar, 62.5Mvar at 100% to 25% *RL load.*

Maximum values of fluctuations of P_{SYN} and Q_{SYN} are 80MW and 120Mvar respectively. Its steady state values are 188.4MW, 130.8MW, 81.66MW, 35.12MW and 292.2Mvar, 186.2Mvar, 79.99Mvar, -39.8Mvar at 100% to 25% *RL load* respectively. Settling time of P_{SYN} and Q_{SYN} at various *RL load* conditions are different, that is, 3.2sec, 3.7sec, 4.0sec for P_{SYN}. Q_{SYN} is consumed by the synchronous generator at 25% load.

During the initial state, P_{SEIG} and Q_{SEIG} are -245MW and -408Mvar at 25% load. 2.0sec is the settling time of P_{SEIG} and Q_{SEIG} which is similar to the previous cases I, II, III of the SEIG. 102.0MW, 102.2MW, 102.5MW, 102.6MW and -60.41Mvar, -60.04Mvar, -59.71Mvar, -59.38Mvar are the normal values of P_{SEIG} and Q_{SEIG} at full load to 25% load. At this various stages of the load, only P_{SEIG} contributes to the load by the SEIG and its values are from 102.0MW to 102.6MW and Q_{SEIG} is consumed by the other interconnected generators.

Based on the performance of the interconnected generators, variations of P_{DFIG} and Q_{DFIG} at the steady state are 2.75MW from 54.26 to 57.01MW and 4.8Mvar from 57.7 to 62.5Mvar. Change in values of DFIG is minimum and consistent. Similarly the contribution of synchronous generator is more than the case II, III. The change in values of P_{SYN} and Q_{SYN} with the different stages of load are 153.28MW from 35.12 to 188.4MW, 332Mvar from -39.8 to 292.2Mvar. At the different stages of this load, P_{SEIG} and Q_{SEIG} steady states are 0.6 MW from 102.0 to 102.6 MW and -1.03 Mvar from -59.38 to -60.41Mvar respectively.

5.5. Case-V: RLC load

Table 5. Real and reactive powers of interconnected generators during RLC load conditions

Load	DFIG				Synchronous Generator				SEIG			
	Initial state (0-0.5sec)		Steady state		Initial state (0-0.5sec)		Steady state		Initial state (0-0.5sec)		Steady state	
	P_{DFIG} (MW)	Q_{DFIG} (Mvar)	P_{DFIG} (MW)	Q_{DFIG} (Mvar)	P_{SYN} (MW)	Q_{SYN} (Mvar)	P_{SYN} (MW)	Q_{SYN} (Mvar)	P_{SEIG} (MW)	Q_{SEIG} (Mvar)	P_{SEIG} (MW)	Q_{SEIG} (Mvar)
25% load	685	380	54.35	63.51	0 to 90	-60 to 90	34.76	-44.92	0 to -243	0 to -412	102.7	-59.53
50% load	685	366	54.63	60.71	0 to 88	-50 to 100	81.39	68.26	0 to -230	0 to -382	102.1	-59.58
75% load	685	350	53.42	60.35	0 to 84	-25 to 106	133.3	168.8	0 to -220	0 to -364	102.0	-59.95
100% load	690	310	50.97	58.07	0 to 80	0 to 110	188.0	259.7	0 to -210	0 to -350	101.9	-60.26

Responses of DFIG, SEIG and synchronous generator at RLC load with 0.8pf are shown in Table 5. At the initial duration of DFIG, peak values of P_{DFIG} and Q_{DFIG} are 690MW at full load and 380Mvar at 25% *RLC load*. It is noted that, the steady state values of P_{DFIG} and Q_{DFIG} are 50.97MW, 53.42MW, 54.63MW, 54.35MW and 58.07Mvar, 60.35Mvar, 60.71Mvar, 63.51Mvar with respect to *RLC load* from full load to 25% load with 0.8pf.

Peak values of P_{SYN} and Q_{SYN} at the initial period are 90MW at 25% of full load and 110 at full load. 188.0MW, 133.3MW, 81.39MW, 34.76MW and 259.7Mvar, 168.8Mvar, 68.26Mvar, -44.92Mvar are the $P_{SYN,}$ and Q_{SYN} normal values during the running and contribution of *RLC load* with the different cases by the interconnected synchronous generator.-44.92Mvar is the consumption of Q_{SYN} by the synchronous generator from the interconnected system only at 25% *RLC load*.

P_{SEIG} and Q_{SEIG} of the SEIG at the starting stages are -243MW and -412Mvar respectively and normal

state values of the P_{SEIG} and Q_{SEIG} with 100% to 25% *RLC load* are 101.9MW, 102.0MW, 102.1MW, 102.7MW and -60.26Mvar, -59.95Mvar, -59,58Mvar, -59.53Mvar respectively.
At the RLC load with 0.8pf, variations of P_{DFIG} and Q_{DFIG} at the different stages of RLC load are 4.65MW from 53.42 to 58.07MW, 5.44Mvar from 58.07 to 63.51Mvar. Synchronous generator shares more load than the DFIG at 50% to full load and less than at 25% load. Changes in values of P_{SYN} and Q_{SYN} are 153.24MW from188.0 to 34.76MW and 304.62Mvar from 259.7 to -44.92Mvar respectively. Similarly in the SEIG performance at RLC load condition, changes in values of P_{SEIG} and Q_{SEIG} are 0.8MW from 101.9 to 102.7MW, -0.73Mvar from -59.53 to -60.26Mvar.
Based on the above analysis, the overall performance of the vector controlled DFIG, SEIG and synchronous generators with *R, L, C, RL, RLC load* are discussed. In all the load conditions, P_{DFIG} and Q_{DFIG} are almost similar. Q_{SYN} is consumed by the synchronous generator from asynchronous generators and the contribution of P_{SYN} is also minimum at inductive and capacitive loads. Other than these loads, it is noted that, the steady state values of P_{SYN} and Q_{SYN} are more than the DFIG. Settling time of P_{SYN} and Q_{SYN} varies with respect to different load conditions. In all the load conditions, Q_{SEIG} is consumed from other generators and it delivers P_{SEIG} to the load. From the SEIG responses, the steady states of P_{SEIG} and Q_{SEIG} are reached and it is higher than the DFIG and less than the synchronous generator.

VI. CONCLUSION

The behaviors of DFIG, SEIG with the hydro governor synchronous generator under various load conditions had been described. The DFIG had consistent performance at all the load conditions because the contribution of P_{DFIG} and Q_{DFIG} values are almost same at *R, L, C, RL, RLC loads*. But in *L* and *C* loads, poor performances are obtained from the synchronous generator, that is, Q_{SYN} is consumed from other interconnected system and contribution of P_{SYN} is small in vice-versa. The better behavior could be achieved by the synchronous generator at *R, RL, RLC loads*. Quality of SEIG is pointed out; where it always consumes Q_{SEIG} and delivers P_{SEIG} to the load. Based on the above discussion, the following points are summarized. Q_{SEIG} is consumed by SEIG. If suitable value of excitation capacitor bank is connected at the stator terminal of SEIG, then, consumption of Q_{SEIG} from the interconnected system will be avoided. At *L* and *C* loads, P_{SYN} delivered to the load by synchronous generator is minimum and Q_{SYN} is consumed from the interconnected system. Simulation studies have showed that, DFIG is recommended for getting the uniform responses such as P_{DFIG} and Q_{DFIG} than the other generators at all the load conditions and better performance and load sharing is achieved by DFIG than SEIG and synchronous generator.

VII. FUTURE WORK

Designing various DFIG controllers such as proportional-integral (PI), direct power (DP), direct torque (DT) controllers and incorporating those controllers in the rotor circuit of DFIG. Analysis can be done on the performance behavior of those controllers in the isolated DFIG system. And also, analysis the impact of those DFIG controllers can be done in the interconnected grid system.

APPENDIX

DFIG parameters

Rated power	: 119.98[MVA]
Rated Voltage (L-L)	: 13.8 [KV]
Base Angular Velocity	: 376.99 [rad/s]
Stator/Rotor Turns Ratio	: 2.637687
Angular Moment of Inertia (J=2H)	: 0.7267 [s]
Mechanical Damping	: 0.001 [p.u.]

SEIG parameters

Rated RMS Phase Voltage	: 7.967 [KV]
Rated RMS Phase Current	: 5.02 [KA]

Base Angular Frequency : 50.0 [Hz]
Polar Moment of Inertia (J=2H) : 5 [s]
Mechanical Damping : 0.008 [p.u.]

Synchronous Generator parameters

Rated RMS Line-to-Neutral voltage(V_{rms}) : 7.967 [KV]
Rated RMS Line current (I_{rms}) : 5.02 [KA]
Base Angular Frequency (ω) : 376.991[rad]
Inertia Constant (H) : 3.117[s]
Mechanical Friction and windage (D_m) : 0.04 [p.u.]
Neutral Series Resistance (R_s) : 1.0E5[p.u.]
Neutral Series Reactance (X_s) : 0 [p.u.]
Iron Loss Resistance (R_m) : 300.0 [p.u.]

REFERENCES

[1] Goutham. D, Vittal. V, "Impact of DFIG based wind turbine generators on transient and small signal stability of power systems", IEEE Conference on Power and Energy Society, 26-30, July 2009, pp. 1-6, ISSN: 1944-9925.
[2] M.T. Abolhassani, H.A. Toliyat, P. Enjeti, "Stator flux-oriented control of an integrated alternator/active filter for wind", *Proceedings of the IEEE International Electric Machines and Drives Conference*, Vol.1, 1-4 June, 2003, pp.461-467.
[3] Eel-Hwan, Sung-Bo Oh, Yong-Hyun Kim, Chang-Su Kim, "Power Control of Doubly Fed Induction Machine without Rotational Transducers", *Proceedings of the 2000 Power Electronics and Motion Control Conference*, Vol. 2, 15-18 August 2000. pp.951-955.
[4] H. Azaza, A. Masmoudi, "On the Dynamic and Steady State Performance of a Vector Controlled DFM Drive Systems", *IEEE International Conference on Man and Cybernetics*, Vol. 6, 6-9 October 2002.
[5] A. Tapia, G. Tapia, J.X. Ostolaza, J.R. Saenz, "Modelling and Control of a Wind Turbine driven DFIG, *IEEE Trans. Energy Convers*. 18(2), 2003, pp.194-204.
[6] Yi Wang and Lie Xu, "Coordinated Control of DFIG and FSIG-Based Wind Farms Under Unbalanced Grid Conditions", *IEEE Trans. on Power Delivery*, Vol. 25, No. 1, Jan 2010, pp. 367-377.
[7] T.F. Chan, "Self-excited Induction Generators Driven by Regulated and Unregulated Turbines", *IEEE Trans. on Energy Conversion*, June 1996, Vol. 11, No. 2, pp. 338-343.
[8] K.E. Hallenius, P Vas, J.E. Brown., "The Analysis of a Saturated Self-Excited Asynchronous Generator", *IEEE Trans.Energy Conversion*, June 1991, Vol. 6, No. 2, pp. 336-345.
[9] Ong CM, "Dynamic Simulation of electric machinery using MATLAB/SIMULINK", Prentice Hall, 1998.
[10] Gil D. Marques and Duarte M. Sousa "New Sensorless Rotor Position Estimator of a DFIG Based on Torque Calculations-Stability Study", *IEEE Trans. on Energy Conversion*, Vol. 27, No. 1, March 2012.
[11] Adeola Balogun, Olorunfemi Ojo, Frank Okafor, and Sosthenes Karugaba, "Determination of Steady-State and Dynamic Control Laws of Doubly Fed Induction Generator Using Natural and Power Variables", *IEEE Trans. Industrial. Applications*, Vol. 49, No. 3, May/June 2013.
[12] Castro, L.M, .Fuerte-Esquivel, C.R. ; Tovar-Hernandez, J.H., "Solution of Power Flow With Automatic Load-Frequency Control Devices Including Wind Farms", *IEEE Trans. on Power Systems*, Vol.27 , Issue 4, pp. 2186 – 2195, 2012.
[13] J. Morren , J. Pierik and S. W. H. de Haan, "Inertial response of variable speed wind turbines", *Elect. Power Syst. Res.*, VOL. 76, No. 11, pp.980 -987, 2006.
[14] P. Kundur, "Power System Stability and Control", McGraw Hill Inc., 1994.
[15] Deane. P, McKeogh, E ; Gallachoir, B.P.O., "Derivation of Inter temporal Targets for Large Pumped Hydro Energy Storage With Stochastic Optimization", IEEE Transactions on Power Systems, Vol.28, Issue: 3, pp. 2147 – 2155, 2013.
[16] R. H. Salim , R. Kuiava , R. A. Ramos and N. G. Bretas "Impact of power factor regulation on small-signal stability of power distribution systems with distributed synchronous generators", *Eur. Trans. Elect. Power*, vol. 21, No. 7, pp.1923 -1940 2011.
[17] P.M. Anderson, Anjan Bose, Stability Simulation Of Wind Turbine Systems, *Transactions on Power Apparatus And Systems*. Vol. PAS 102, No. 12, December 1983, pp. 3791-3795.
[18] Murdoch, A., Winkelman, J.R. ; Javid, S.H. ; Barton, R.S, "Control Design and Performance Analysis Of A

6 Mw Wind Turbine Generator", *IEEE Transactions On Power Apparatus and Systems*, Vol. PAS 102, No. 5, May 1983, pp. 1340-1347.

AUTHORS

A. Ramkumar received the M.E (Power Systems) degree from Faculty of Engineering and Technology, Annamalai University, Chidambaram, TamilNadu, India, in 2002 and received B.E (Electrical and Electronics Engineering) degree from Thiagarajar College of Engineering, Madurai Kamarajar University, Madurai, TamilNadu, India in 1997. He has been working as Assistant Professor in the Department of Electrical and Electronics Engineering, Kalasalingam University, Srivilliputhur, TamilNadu, since 2003. His research interests include Electrical Machines, Power System Analysis, High Voltage DC transmission Systems, Reactive Power Compensation, Flexible AC transmissions Systems and Power System Automation.

S. Durairaj received Ph.D degree from Madurai Kamaraj University in 2006 and received BOYSCAST FELLOWSHIP from DST, Govt. of India for the year 2006-2007 for doing post-doctoral research at Queens University Belfast, UK. He received Young Scientist Fellowship (YSF) for the year 2002 from Tamilnadu State Council for Science and Technology (TNSCST) undergone training in Asia Brown Boweri (ABB) Ltd., Bangalore, India in the area of power system automation. He worked as a Professor in the Department of Electrical and Electronics Engineering, Kalasalingam University, Srivilliputhur, TamilNadu, India from 1996 to 2013. Now he is working as a Professor in the Department of Electrical and Electronics Engineering, Kings College of Engineering, Tanjore, TamilNadu, India. His research interests include Reactive Power Management, Distribution Automation, Energy Conservation and Energy Management Systems.